Magnetoconductivity of quantum wires with elastic and inelastic scattering

Henrik Bruus
Applied Physics, Yale University, P.O. Box 2157, New Haven, Connecticut 06520

Karsten Flensberg
Nordita, Blegdamsvej 17, Copenhagen 2100 Ø, Denmark

Henrik Smith
Niels Bohr Institute, Ørsted Laboratory, Universitetsparken 5, Copenhagen 2100 Ø, Denmark

We use a Boltzmann equation to determine the magnetoconductivity of quantum wires. The presence of a confining potential in addition to the magnetic field removes the degeneracy of the Landau levels and allows one to associate a group velocity with each single-particle state. The distribution function describing the occupation of these single-particle states satisfies a Boltzmann equation, which may be solved exactly in the case of impurity scattering. In the case where the electrons scatter against both phonons and impurities we solve numerically—and in certain limits analytically—the integral equation for the distribution function and determine the conductivity as a function of temperature and magnetic field. The magnetoconductivity exhibits a maximum at a temperature, which depends on the relative strength of the impurity and electron-phonon scattering and shows oscillations when the Fermi energy or the magnetic field is varied.

I. INTRODUCTION

The possibility of making quasi-one-dimensional quantum wires, due to advances in microfabrication technology, has greatly stimulated the interest in the transport properties of such low-dimensional systems. A number of recent papers have treated the magnetoconductivity of quantum wires[1] using a variety of different theoretical approaches. The suppression of scattering between edge states, due to the presence of the magnetic field, was discussed by several authors.[2-4] The effects of impurity and boundary scattering on the Hall effect in quantum wires were treated by Akera and Ando,[5] starting from a Boltzmann equation. The Kubo method[6] has been used for considering the effect of the coupling to optical phonons[7,8] and the influence of impurity scattering[9] on the magnetotransport through quantum wires. Momentum- and energy-balance equations have been derived[10,11] for a quasi-one-dimensional gas of electrons in a magnetic field. Other authors[12] have used the Keldysh method to discuss magnetotransport in the presence of impurity scattering, while the formalism due to Landauer[13] and Büttiker[14] was employed in Ref. 15 to treat the influence of disorder on the Hall effect in quantum wires.

Transport in strong magnetic fields has traditionally been treated within the Kubo formalism, since this allows one to take fully into account the quantization of the motion of an electron in a magnetic field. The resulting diagrammatic expansion of the conductivity requires the consideration of both self-energy effects and vertex corrections. It was demonstrated in Ref. 9 that it is essential to include vertex corrections in order to determine the effect of impurity scattering on the magnetoconductivity of a quantum wire. The physical reason for this is that only backscattering from the impurities contributes to the resistivity.

In the present paper we use a Boltzmann equation to determine the transport properties of quantum wires formed by additional confinement of the two-dimensional electron gas of, e.g., a GaAs-GaAlAs heterojunction. The presence of a confining potential in addition to the magnetic field removes the degeneracy of the Landau levels and allows one to associate a group velocity with each single-particle state. The distribution function describing the occupation of these single-particle states satisfies a Boltzmann equation, which we solve exactly in the case of impurity scattering. The resulting magnetoconductivity agrees with that obtained in Ref. 9 within the Kubo approach. In the case of electron-phonon scattering we solve numerically—and in certain limits analytically—the integral equation for the distribution function. The conductivity is determined as a function of temperature and magnetic field in the case when both impurities and phonons contribute to the scattering of the electrons. Our paper extends previous work discussed above by giving a more complete account of the simultaneous influence of electron-impurity and electron-phonon scattering. By starting from the Boltzmann equation we include vertex corrections from the outset, thus simplifying the formal development in comparison to that involved in the use of the Kubo formalism.

Apart from its simplicity, the use of the Boltzmann equation has the additional advantage that it allows one to go beyond linear-response theory in a straightforward manner. Although the present paper treats in detail only

<u>48</u>   11 144

the regime of linear response, our approach may readily be generalized to take nonlinear effects into account.

Since conduction in a quantum wire involves current transport in one dimension, it is necessary to consider the role of localization. This was done in Ref. 16, where it was shown that weak localization in quantum wires is destroyed in a magnetic field greater than a critical value B_c, where the critical magnetic field B_c apart from numerical factors is given by $B_c \simeq \hbar \ell / e L_\phi W^2$. Here ℓ is the elastic scattering length, W is the width of the quantum wire, while L_ϕ is the phase coherence length. For the parameters considered in Ref. 16 this yields a B_c somewhat less than 0.1 T. In what follows we shall assume that the magnetic field is sufficiently strong that localization effects are always negligible. The transport properties of the quantum wires may then be obtained from a Boltzmann equation, in which the quantizing effect of the magnetic field is incorporated in the manner described below. We shall also disregard Coulomb-blockade effects which have been shown to be of importance in some systems.[17]

The paper is organized as follows. In Sec. II we introduce the single-particle states derived from the presence of a confining potential in addition to a homogeneous magnetic field. The Boltzmann equation and its solution are discussed in Sec. III. In Sec. IV we treat scattering due to impurities, while scattering from impurities and acoustical phonons forms the subject of Sec. V, where we consider both deformation-potential and piezoelectric coupling. Finally Sec. VI deals with the case where scattering from impurities and optical phonons is important.

II. THE SINGLE-PARTICLE ENERGY SPECTRUM

We consider an electron moving in the xy plane under the influence of a constant magnetic field in the z direction. In addition a parabolic confinement potential limits its motion in the y direction whereby a wire is formed in the x direction. The Hamiltonian for such an electron is

$$\hat{H} = \frac{1}{2m^*}(\mathbf{p} + e\mathbf{A})^2 + \frac{1}{2}Ky^2, \tag{1}$$

m^* being the effective (band) mass of the electron. For simplicity we have neglected the Zeeman splitting, since we shall be mainly concerned with quantum wires in GaAs-based structures, where the Zeeman energy is a few percent of the cyclotron energy $\hbar \omega_c$ to be defined below. The electron spin therefore only enters as a factor of 2 in the expression for the current density. In the x direction we impose periodic boundary conditions, and for the vector potential $\mathbf{A}$ we use the Landau gauge $\mathbf{A} = B(-y, 0, 0)$. Consequently the eigenfunctions of the Hamiltonian are products of plane waves and harmonic-oscillator functions involving Hermite polynomials H_n,

$$\Psi_{nk}(x, y) = \frac{1}{\sqrt{L}} e^{ikx} \frac{1}{(\sqrt{\pi} 2^n n! \ell_h)^{1/2}}$$
$$\times H_n \left(\frac{y - y_k}{\ell_h}\right) \exp\left(-\frac{(y - y_k)^2}{2\ell_h^2}\right), \tag{2}$$

with L being the length of the quantum wire. The center coordinate y_k and the characteristic length ℓ_h of the harmonic oscillator are specified below. The wave function in the z direction is taken to be a δ function.

In the case where K is zero and only the magnetic field is present the natural system of units is based on the cyclotron frequency ω_c and the magnetic length ℓ_c, given by

$$\omega_c = \frac{eB}{m^*}, \qquad \ell_c^2 = \frac{\hbar}{eB}. \tag{3}$$

When K is different from zero, we define the quantity γ, which describes the relative strength of the confinement potential, by

$$\gamma \equiv \frac{K}{m^* \omega_c^2}, \tag{4}$$

and the natural units are now based on the hybrid frequency ω_h and the hybrid characteristic length ℓ_h given by

$$\omega_h = (1 + \gamma)^{\frac{1}{2}} \omega_c, \qquad \ell_h = (1 + \gamma)^{-\frac{1}{4}} \ell_c. \tag{5}$$

By inserting the function (2) in the Schrödinger equation

$$\hat{H}\Psi_{nk} = \varepsilon_{nk}\Psi_{nk}, \tag{6}$$

one finds that (6) is satisfied, provided

$$\varepsilon_{nk} = \hbar \omega_h \left(n + \frac{1}{2}\right) + \frac{\hbar^2 k^2}{2m}, \quad n = 0, 1, 2, \ldots, \tag{7}$$

where m is a renormalized mass defined by

$$m = \frac{1 + \gamma}{\gamma} m^*. \tag{8}$$

The center of the harmonic-oscillator wave functions is given by

$$y_k = \frac{\omega_c \hbar k}{m^* \omega_h^2} = (1 + \gamma)^{-\frac{1}{2}} k \ell_h^2. \tag{9}$$

The confinement potential $Ky^2/2$ removes the degeneracy of the Landau levels through the k dependence exhibited in (7). Note that the dispersion relation is that of a free particle with a renormalized mass m. When the strength of the confinement potential goes to zero, the renormalized mass m becomes infinite (corresponding to degenerate Landau levels), while in the opposite limit ($\gamma \to \infty$), the renormalized mass becomes equal to the effective mass m^*. The k-dependent energy levels are plotted in Fig. 1, where we have also indicated the position of the Fermi level corresponding to a definite electron density.

In the following we shall describe conduction through the quantum wire on the basis of the Boltzmann equation for the distribution function of the excitations with energy ε_{nk}. The group velocity v of the excitations is seen to be

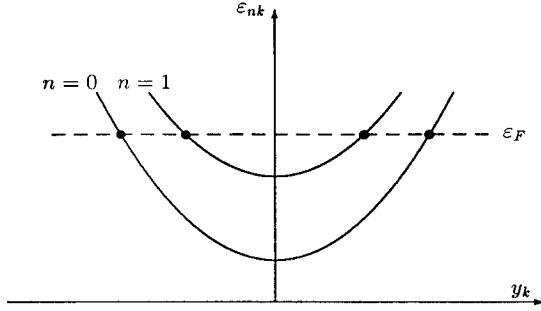$$v_{nk} = \frac{1}{\hbar} \frac{\partial \varepsilon_{nk}}{\partial k} = \frac{\hbar k}{m}. \tag{10}$$

FIG. 1. The two lowest k-dependent energy bands ε_{0k} and ε_{1k} of the quantum wire. The dashed line represents an arbitrary Fermi level above the bottom of the second band.

If the confinement potential is not simply parabolic, the relation between v_{nk} and k becomes more complicated than Eq. (10), but the method described in the following is still applicable, provided one modifies the group velocity accordingly, and incorporates the new wave functions into the matrix elements appearing in the collision probability.

III. THE BOLTZMANN EQUATION

We consider the distribution function f_{nk} for the excitations specified by the energy ε_{nk}, with group velocity $v_{nk} = \hbar k/m$. Unlike the usual semiclassical description of transport in a magnetic field, the magnetic field has here been taken into account from the very beginning, in defining the excitations with dispersion relation (7). The effect of an electric field E_x in the x direction is, however, included in the usual manner through the acceleration equation

$$\hbar \dot{k} = -eE_x. \tag{11}$$

The Boltzmann equation[18] is

$$\frac{\partial f_{nk}}{\partial t} + \dot{k} \frac{\partial f_{nk}}{\partial k} = \left(\frac{\partial f_{nk}}{\partial t}\right)_{\text{coll}}, \tag{12}$$

where the right-hand side of the equation contains the collision term. Since we are interested in the linear response to a static electric field, the time derivative $\partial f/\partial t$ is equal to zero, while f_{nk} in the second term on the left-hand side may be replaced by the equilibrium function f_{nk}^0. Using Eq. (11) the Boltzmann equation then becomes an inhomogeneous integral equation of the form

$$\frac{eE_x}{k_B T} v_{nk} f_{nk}^0 (1 - f_{nk}^0) = \left(\frac{\partial f_{nk}}{\partial t}\right)_{\text{coll}}, \tag{13}$$

with the integral term on the right-hand side—the collision term—to be specified below.

Before we consider specific scattering mechanisms, let us write down the conductivity σ in terms of the distribution function. In the present work we define σ as $\sigma \equiv j_x/E_x$, j_x being the current density in the x direction. In terms of the two-dimensional resistivity tensor ρ

we get $\sigma = 1/\rho_{xx}$ because $j_y = 0$. However, in the presence of the magnetic field a current in the x direction will also induce an electric field in the y direction. This Hall response will be dealt with in a future publication. For j_x we have

$$j_x = -2e \sum_n \int_{-\infty}^{\infty} \frac{dk}{2\pi} v_{nk} f_{nk}. \tag{14}$$

We shall introduce the deviation function ψ_{nk} by the definition

$$f_{nk} \equiv f_{nk}^0 + f_{nk}^0 (1 - f_{nk}^0) \psi_{nk}. \tag{15}$$

Then the current density becomes

$$j_x = -2e \sum_n \int_{-\infty}^{\infty} \frac{dk}{2\pi} v_{nk} f_{nk}^0 (1 - f_{nk}^0) \psi_{nk}. \tag{16}$$

Since we shall be dealing with distribution functions that change sign upon $k \to -k$, we may restrict k to positive values and work instead with the distribution function as a function of energy: $\psi_n(\varepsilon)$. In this notation k is then a function of energy, and we denote the k value which solves $\varepsilon = \varepsilon_{nk}$ by $k_n(\varepsilon)$. Furthermore, by introducing the function ϕ_n defined by

$$\phi_n \equiv \frac{k_B T}{eE_x} \psi_n, \tag{17}$$

we may express the conductivity as

$$\sigma \equiv \frac{j_x}{E_x} = \frac{2e^2}{h} 2 \sum_n \int_0^{\infty} d\varepsilon \left(-\frac{\partial f^0(\varepsilon)}{\partial \varepsilon}\right) \phi_n(\varepsilon) \tag{18}$$

since $dk = d\varepsilon/\hbar v$. Note that ϕ has dimension of length. The chemical potential entering the equilibrium distribution function f^0 will be assumed to be independent of temperature, equal to ε_F, since the quantum wire under typical experimental conditions is in contact with a large reservoir of electrons.

The Boltzmann equation considered in this paper is an inhomogeneous integral equation of the form

$$X_{nk} = H\psi_{nk}, \tag{19}$$

where

$$X_{nk} = -\frac{eE_x}{k_B T} v_{nk} f_{nk}^0 (1 - f_{nk}^0), \tag{20}$$

while the integral operator H is defined by

$$\left(\frac{\partial f_{nk}}{\partial t}\right)_{\text{coll}} = -H\psi_{nk} \tag{21}$$

with

$$H\psi_{nk} = \sum_{n'} \int_{-\infty}^{\infty} \frac{L}{2\pi} dk' K_{nn'}(k, k')(\psi_{nk} - \psi_{n'k'}). \tag{22}$$

Here K is an integral kernel to be specified in later sections.

By introducing the scalar product (A, B) through the definition

$$(A, B) = \sum_n \int_{-\infty}^{\infty} \frac{dk}{2\pi} A_{nk} B_{nk} \qquad (23)$$

the conductivity may be written as

$$\sigma = \frac{2k_B T}{E_x^2} (X, \psi). \qquad (24)$$

In cases where we cannot solve explicitly for ψ, it is useful to employ a variational principle, which yields a lower bound on σ by virtue of the Schwarz inequality

$$(\psi, H\psi)(U, HU) \geq (U, H\psi)^2, \qquad (25)$$

where U is an arbitrary trial function. Since $H\psi = X$, this gives a lower bound on the conductivity

$$\sigma \geq \frac{2k_B T}{E_x^2} \frac{(X, U)^2}{(U, HU)}. \qquad (26)$$

This lower bound will be used to determine the low-temperature conductivity when the scattering is due to acoustic phonons, both with and without impurities, and the resulting analytic expressions are compared to the results of the numerical solution of the integral equation.

We shall always write our calculated values of the conductivity, as limited by the various scattering mechanisms to be considered in subsequent sections, in the form

$$\sigma = \frac{2e^2}{h} l, \qquad (27)$$

where l has the dimension of a length. As may be expected, in the presence of impurity scattering l tends to a finite value as T tends to zero, while it increases exponentially in the absence of impurity scattering, when the electrons are scattered only by phonons.

IV. IMPURITY SCATTERING

In this section we consider the case of elastic impurity scattering treated recently in Ref. 9. Our aim is to show how the results of Ref. 9, which were obtained by use of the Kubo formalism, are derived within the present framework. The collision integral is

$$\left(\frac{\partial f_{nk}}{\partial t}\right)_{\text{coll}} = -\sum_{n'} \int_{-\infty}^{\infty} \frac{L}{2\pi} dk' w_{nn'}(k, k')(f_{nk} - f_{n'k'}),$$
$$(28)$$

since the scattering is elastic. According to the golden rule we have

$$w_{nn'}(k, k') = \frac{2\pi}{\hbar} |\langle nk|V|n'k'\rangle|^2 \delta(\varepsilon_{nk} - \varepsilon_{n'k'}). \qquad (29)$$

The square of the matrix element $\langle nk|V|n'k'\rangle$ for scattering from impurities may be written as

$$|\langle nk|V|n'k'\rangle|^2 = \int d^2r \int d^2r' V(\mathbf{r})V(\mathbf{r}')$$
$$\times \langle nk|\mathbf{r}\rangle \langle \mathbf{r}|n'k'\rangle \langle n'k'|\mathbf{r}'\rangle \langle \mathbf{r}'|nk\rangle. \qquad (30)$$

We shall perform an ensemble average over the distribution of impurities, corresponding to the replacement

$$V(\mathbf{r})V(\mathbf{r}') \rightarrow \langle V(\mathbf{r})V(\mathbf{r}')\rangle = F(\mathbf{r}, \mathbf{r}'). \qquad (31)$$

When the impurity potential may be approximated by a δ function in space, the function F is proportional to the δ function $\delta(\mathbf{r} - \mathbf{r}')$, corresponding to a "white-noise" model

$$F(\mathbf{r}, \mathbf{r}') = A^2 n_{\text{imp}} \delta(\mathbf{r} - \mathbf{r}'). \qquad (32)$$

Here we have introduced the number of impurities per unit area n_{imp} together with the constant A, which denotes the magnitude of the matrix element for scattering from a single impurity. The dimension of A is that of an energy times an area.

In order to distinguish between states of equal energy but opposite sign of k, we introduce the "branch index" $s = \pm 1$:

$$k_{ns}(\varepsilon) \equiv sk_n(\varepsilon) = s\sqrt{\frac{2m}{\hbar^2}[\varepsilon - (n + \tfrac{1}{2})\hbar\omega_h]}, \qquad (33)$$

provided

$$(n + \tfrac{1}{2})\hbar\omega_h \leq \varepsilon. \qquad (34)$$

The density of states at the Fermi energy ε_F is inversely proportional to the s-independent Fermi velocity $v_n(\varepsilon_F) = \frac{\hbar}{m} k_n(\varepsilon)$. Finally, since ϕ_{ns} is odd in k and hence changes sign with s, we may write $\phi_{ns} = s\phi_n$. The problem then becomes that of solving the matrix equation

$$s = \sum_{n's'} B_{ns}^{n's'} (s\phi_n - s'\phi_{n'}), \qquad (35)$$

and calculating the conductivity according to Eq. (18). The matrix $B_{ns}^{n's'}$ is positive and symmetric with respect to interchange of ns with $n's'$. Its elements are

$$B_{ns}^{n's'} = \frac{1}{\hbar^2} A^2 n_{\text{imp}} \frac{1}{v_n v_{n'}} \frac{1}{\ell_h \sqrt{2\pi}} F_{ns}^{n's'}. \qquad (36)$$

Here we have defined the following dimensionless quantities:

$$F_{ns}^{n's'} = \sqrt{2\pi} \, \ell_h \int_{-\infty}^{\infty} dy |u_n(y - y_{k_{ns}})|^2 |u_{n'}(y - y_{k_{n's'}})|^2,$$
$$(37)$$

where $u_n(y)$ is the normalized y-dependent part of the wave function (2). The overlap integral $F_{ns}^{n's'}$ has the form $P_{ns}^{n's'}(z) e^{-z}$, where $P_{ns}^{n's'}(z)$ is a polynomial in z, and where $z = (y_{k_{ns}} - y_{k_{n's'}})^2/(2l_h^2)$.

In Fig. 2 we show the result of solving the matrix equation (35) and calculating the conductivity according to Eq. (18) as a function of the Fermi energy ε_F, for differ-
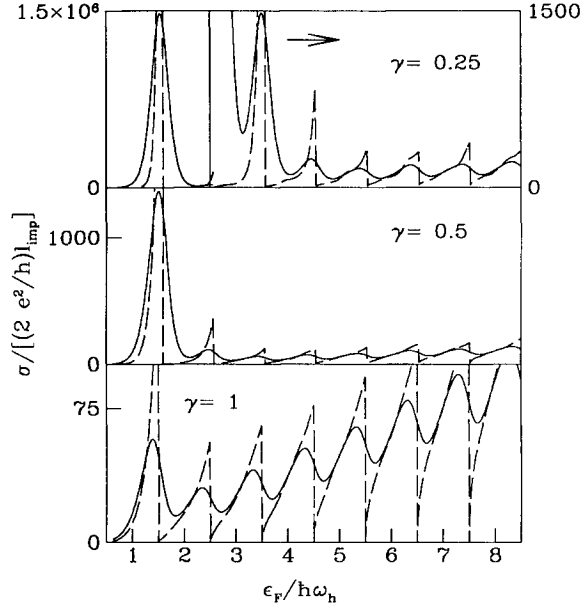
FIG. 2. The conductivity for a quantum wire with impurity scattering plotted vs the Fermi level for three different choices of the confinement potential corresponding to $\gamma = 1$, 0.5, and 0.25. The dashed line is the $T = 0$ result and the solid lines correspond to $k_B T = 0.05\hbar\omega_h$. The magnetic field is 9 T.

ent choices of the parameter γ determining the strength of the confining potential. As can be seen in the figure the conductivity rises quickly as the Fermi level increases above $\frac{1}{2}\hbar\omega_h$. This is due to the increasing separation between the two edge states, expressed by the overlap integral F_{0-}^{0+} of Eq. (37) which leads to the exponential factor in Eq. (38) below. When ϵ_F hits the next Landau level (cf. Fig. 1), the conductivity starts to decrease because a channel for backscattering is opened, i.e., the $n = 0$ edge state can scatter to the opposite edge through the $n = 1$ edge states. However, when the $n = 1$ edge states become decoupled, the conductivity starts to increase again. This qualitative behavior is repeated each time a new Landau

level crosses the Fermi level. The height of the conductance peak at $\frac{3}{2}\hbar\omega_h$ increases strongly with increasing channel width. At finite temperature these features are somewhat smeared, as evidenced by the figure, but still clearly visible.

Our calculation is relevant for the case where the scattering between different channels is so strong that the Boltzmann picture is valid, in other words, the calculated mean free path must be considerably shorter than the length of the wire. In the high magnetic field limit this means that the wire may not be so broad that the edge states become decoupled. Thus in practice we are dealing with wires only a few times l_h wide.

When $\hbar\omega_h/2 \leq \varepsilon_F \leq 3\hbar\omega_h/2$ only the lowest Landau level is involved, corresponding to $n = n' = 0$ in Eq. (35). Then the solution becomes particularly simple, $\phi_0 = 1/2B_{0+}^{0-}$. By means of the Sommerfeld expansion we obtain the following low-temperature expression for the conductivity $\sigma = 2e^2/hB_{0+}^{0-}$,

$$\sigma = \frac{2e^2}{h} l_h \sqrt{2\pi} \frac{\hbar^2}{A^2 n_{\text{imp}}} \frac{\hbar^2 k_F^2}{m^2} \exp\left(2k_F^2 l_h^2/[1+\gamma]\right)$$
$$\times \left[1 + \frac{8\pi^2}{3\gamma^2}\left(1 + \frac{1+\gamma}{k_F^2 l_h^2}\right)\left(\frac{k_B T}{\hbar\omega_h}\right)^2\right], \qquad (38)$$

where $k_F = k_{0+}(\varepsilon_F)$ is the Fermi momentum. The conductivity increases with temperature because electrons are excited into states which have a smaller overlap with the states at the opposite branch. Consequently the electrons have a smaller backscattering probability. The result (38) is valid only to lowest order in $(k_B T/\hbar\omega_h)^2$. In obtaining our numerical results we do not use the Sommerfeld expansion, but calculate directly the integral over energy according to the expression (18).

As an illustration of the matrix inversion involved in the solution of the Boltzmann equation we shall also give the expression for the zero-temperature conductivity in the case when $3\hbar\omega_h/2 \leq \varepsilon_F \leq 5\hbar\omega_h/2$. By utilizing the symmetry $\phi_{n+} = -\phi_{n-}$ the 4×4 matrix equation becomes a 2×2 equation which may readily be solved for ϕ_{0+} and ϕ_{1+}. The resulting conductivity $\sigma = (2e^2/h)2(\phi_{0+} + \phi_{1+})$ is at $T = 0$ K given by

$$\sigma = \frac{2e^2}{h} \frac{2(2B_{0+}^{1+} + B_{1+}^{1-} + B_{0+}^{0-})}{2(B_{0+}^{1+}B_{0+}^{1-} + B_{0+}^{0-}B_{1+}^{1-}) + (B_{0+}^{1+} + B_{0+}^{1-})(B_{0+}^{0-} + B_{1+}^{1-})}. \qquad (39)$$

The result (39) yields the conductivity at zero temperature, when the Fermi energy ε_F satisfies the condition $3\hbar\omega_h/2 \leq \varepsilon_F \leq 5\hbar\omega_h/2$, in agreement with Ref. 9. The generalization to more Landau levels is straightforward. The B matrix in Eq. (35) is in general a $2(n_0 + 1) \times 2(n_0 + 1)$ matrix given by Eq. (36), where n_0 is the quantum number associated with the highest occupied Landau level at $T = 0$ K.

It is convenient to relate the conductivity calculated in the following two sections to the zero-temperature conductivity σ_{2D} associated with motion in two dimensions

in the absence of a magnetic field and a confinement potential. The latter is given by

$$\sigma_{2D} = \frac{e^2 n_{2D}}{m^*}\tau_{\text{imp}} = en_{2D}\mu_{\text{imp}}, \qquad (40)$$

where n_{2D} is the electron sheet density and μ_{imp} is the zero-field, zero-temperature mobility,

$$\mu_{\text{imp}} = \frac{e\tau_{\text{imp}}}{m^*} \qquad (41)$$

with

$$\frac{1}{\tau_{\text{imp}}} = \frac{m^* A^2 n_{\text{imp}}}{\hbar^3}.$$ (42)

We shall thus express our calculated conductivity in units of $(2e^2/h)l_{\text{imp}}$, where

$$l_{\text{imp}} = \tau_{\text{imp}} \omega_c l_c$$ (43)

is a characteristic length which depends on the impurity content as well as the magnetic field.

V. ELECTRON-PHONON SCATTERING

Next we turn to the consideration of inelastic processes. The present section treats the case where the electrons are scattered by acoustical phonons due to the combined deformation potential and piezoelectric coupling, while the following section discusses the coupling of electrons to optical phonons.

Before specializing to a particular model let us write down the contribution to the collision operator from the scattering against phonons. The phonons are assumed to be in thermal equilibrium. Then the integral operator H is given by the following expression:

$$H\psi_{nk} = \frac{2\pi}{\hbar} \sum_{n'} \sum_{k'} \sum_{\mathbf{q}} |g_{\mathbf{q}}|^2 f^0(\varepsilon_{nk})[1 - f^0(\varepsilon_{n'k'})]\delta_{k,k'+q_x}(\psi_{nk} - \psi_{n'k'})$$

$$\times \{\delta(\varepsilon_{n'k'} - \varepsilon_{nk} + \hbar\omega_q)[1 + N^0(\omega_q)] + \delta(\varepsilon_{n'k'} - \varepsilon_{nk} - \hbar\omega_q)N^0(\omega_q)\}.$$ (44)

Here $g_{\mathbf{q}}$ is the electron-phonon coupling parameter, which will be specified below, while $N^0(\omega_q)$ is the equilibrium phonon distribution. For simplicity we have assumed that the phonon frequencies only depend on the magnitude of $\mathbf{q}$. In Eq. (44) we have explicitly written the factor $\delta_{k,k'+q_x}$ discussed in the Appendix. Utilizing the relationship

$$f(\varepsilon)[1 - f(\varepsilon \pm \hbar\omega_q)] = [f(\varepsilon) - f(\varepsilon \pm \hbar\omega_q)][1 + N^0(\pm\omega_q)],$$ (45)

the collision integral (44) can be written as

$$H\psi_{nk} = \frac{2\pi}{\hbar} \sum_{n'q\sigma} |g_{\mathbf{q}}|^2 \frac{|f^0(\varepsilon_{nk}) - f^0(\varepsilon_{nk} + \sigma\hbar\omega_q)|}{4\sinh^2(\hbar\omega_q/2k_BT)}$$

$$\times (\psi_{nk} - \psi_{n'k-q_x})\delta(\varepsilon_{n'k-q_x} - \varepsilon_{nk} - \sigma\hbar\omega_q),$$ (46)

with σ assuming the two values $+1$ and -1 corresponding to phonon absorption and emission, respectively.

Our calculations of $g_{\mathbf{q}}$ are based on the standard electron-phonon interaction Hamiltonian, which disregarding umklapp processes takes the form

$$\hat{H}_{ep} = \sqrt{\frac{\hbar}{2V\rho\omega_q}} \sum_{\lambda,\mathbf{q}} M_\lambda(\mathbf{q})\hat{\rho}(\mathbf{q})(\hat{a}_{\mathbf{q}} + \hat{a}^\dagger_{-\mathbf{q}}),$$ (47)

where ρ is the ion mass density, V the normalization volume, $\hat{\rho}(\mathbf{q})$ the Fourier component of the electron density operator, $\hat{a}^\dagger_{-\mathbf{q}}$ a phonon creation operator, and λ the polarization index. The coupling function M is given by

$$M_\lambda(\mathbf{q}) = -V(\mathbf{q})\,\mathbf{q}\cdot\boldsymbol{\xi}_\lambda,$$ (48)

$V(\mathbf{q})$ being the electron-ion potential and $\boldsymbol{\xi}_\lambda$ a unit vector describing the polarization λ. For a detailed treatment of electron-phonon coupling in semiconductors see, e.g., Ref. 19. The values of the GaAs parameters used in our calculations are listed in Table I.

A. Coupling to acoustical phonons

In GaAs heterostructures at low temperatures the electron-phonon scattering is mainly due to the combined piezoelectric coupling and the deformation-potential coupling.[20-22] Below we briefly sketch how these couplings are derived.

The deformation potential coupling only involves the longitudinal-acoustical phonons. The coupling to the transverse-acoustical phonons is suppressed by the square of the ratio between the speed of sound and the speed of light. In the long-wavelength limit the coupling function M^{df} for the deformation-potential coupling is written as

$$M^{\text{df}} = \Xi\,q,$$ (49)

where Ξ, known as the deformation potential, is the zero-wave-vector limit of $V(\mathbf{q})$.

The electron-ion potential V for the piezoelectric coupling is found from the basic piezoelectric equations.[19] For GaAs (zinc-blende structure) the only nonvanishing independent piezoelectric constant is h_{14} (reduced nota-

TABLE I. The GaAs constants used in this paper. Unless otherwise indicated the values are taken from Ref. 27.

Parameter	Symbol	Value
Ion mass density	ρ	5.3×10^3 kg m^{-3}
Longitudinal sound velocity	c	5.2×10^3 m s^{-1}
Transverse sound velocity	xc	3.0×10^3 m s^{-1}
Sound velocity ratio	x	0.58
Static dielectric constant	κ_0	12.8
High-frequency dielectric constant	κ_∞	10.6
Piezoelectric constant (Ref. 23)	h_{14}	1.38×10^9 V m^{-1}
Piezoelectric coupling, Eq. (52)	P	5.4×10^{-20} J^2 m^{-2}
Deformation potential (Ref. 21)	Ξ	2.2×10^{-18} J
Effective electron mass	m^*	$0.067m_0$
Optical-phonon-energy	$\hbar\omega_0$	36 meV

tion), and the coupling function M_λ^{pz} in this case becomes

$$M_\lambda^{pz} = i2eh_{14}(\hat{q}_x\hat{q}_y\hat{\xi}_{\lambda,z} + \hat{q}_y\hat{q}_z\hat{\xi}_{\lambda,x} + \hat{q}_z\hat{q}_x\hat{\xi}_{\lambda,y}), \quad (50)$$

where $\hat{q}_i = (\mathbf{q}/q)_i$ and $\hat{\xi}_{\lambda,i} = (\boldsymbol{\xi}_\lambda)_i$. In the piezoelectric case λ is retained.

It is noted that M^{df} is real while M^{pz} is imaginary; thus to second order the two terms do not interfere, and the absolute square of the total coupling function M^{ac} is given by

$$|M^{ac}|^2 = |M^{df}|^2 + |M^{pz}|^2. \quad (51)$$

To obtain a more tractable form of the piezoelectric coupling we perform angular averages for the longitudinal and the (two) transverse modes separately and then add the terms.[19,23] While this represents an approximation compared to retaining the full $\mathbf{q}$ dependence of the coupling in the collision integral, we expect it to involve only minor quantitative differences. In adding the transverse and longitudinal contribution we must remember the different average sound velocities associated with each of the terms, originating in the factor $1/\sqrt{\omega_q} = 1/\sqrt{cq}$ in Eq. (47). Expressing the transverse sound velocity as x times the longitudinal sound velocity we obtain the following angular average of the absolute square of the piezoelectric coupling function M^{pz}:

$$|M^{pz}|^2 = (eh_{14})^2 \left(\frac{12}{35} + \frac{1}{x}\frac{16}{35}\right) \equiv P, \quad (52)$$

where we have introduced the constant P, and where it is understood that the only sound velocity appearing in the following is the longitudinal one.

The electron-phonon coupling parameter $g_{\mathbf{q}}$ introduced in Eq. (44) now becomes

$$|g_{ac}(q)|^2 = \frac{\hbar}{2\rho Vc}\frac{1}{q}(\Xi^2 q^2 + P)\,|\langle nk|e^{i\mathbf{q}\cdot\mathbf{r}}|n'k'\rangle|^2. \quad (53)$$

The matrix element appearing in this expression is treated in detail in the Appendix. In writing Eq. (53) we have taken the phonon frequency ω_q to be given by

$$\omega_q = cq. \quad (54)$$

B. Coupling to acoustical phonons in the low-temperature limit

In an analytical study of the low-temperature limit we use the variational principle discussed in Sec. III above and choose a trial function given by

$$U = U_{nk} = \text{sgn}(k). \quad (55)$$

Thus U is 1 on the branches corresponding to k being positive, while it is -1 on the branches corresponding to k being negative. This choice will lead to an expression for the conductivity which in the case of a single occupied Landau level and in the limit of low temperature agrees with a numerical solution of the integral equation. This suggests that the trial function is in fact the exact one

under these conditions.

First we evaluate the scalar product (U, X) appearing in the general expression (26) for the lower bound on the conductivity. By changing the integration variable to the energy ε_{nk} we get

$$(X, U) = \frac{eE_x}{\hbar\pi}\sum_n f^0(\varepsilon_{n0}), \quad (56)$$

where ε_{n0} is the $k = 0$ value of ε_{nk}. Because of the symmetry of the integral operator H given in Eq. (46) the denominator occurring in Eq. (26) becomes

$$(U, HU) = \sum_n \int_{-\infty}^{\infty}\frac{dk}{2\pi}\int_{-\infty}^{\infty}\frac{dk'}{2\pi}\sum_{n'}K_{nn'}(k,k')$$
$$\times\frac{1}{2}\left[1 - \text{sgn}(k)\text{sgn}(k')\right]^2. \quad (57)$$

As discussed in the Appendix $k' = k - q_x$. The occurrence of the factor $[1 - \text{sgn}(k)\text{sgn}(k - q_x)]$ in the integrand of Eq. (57) implies that the summation over q_x becomes restricted by $q_x > k$ for $k > 0$, while $q_x < k$ for $k < 0$. Using the symmetry with respect to reversal of all momenta variables we may thus restrict the k integral to the interval 0 to ∞, which limits q_x to the region $q_x > k$. If θ denotes the angle between $\mathbf{q}$ and the x axis, the integration over θ is therefore restricted by

$$\cos\theta > \frac{k}{q}, \quad 0 < q < \infty. \quad (58)$$

Thus we have to carry out three integrations (over q, k, and $\cos\theta$) as well as two sums (over n and n').

Let us consider the simplest case, in which $n = n' = 0$. If the sound velocity is much less than the Fermi velocity then the energy-conserving δ functions are

$$\delta(\varepsilon_{n'k'} - \varepsilon_{nk} \pm \hbar\omega_q) \simeq \delta\left(\frac{\hbar^2}{2m}(q^2\cos^2\theta - 2kq\cos\theta)\right). \quad (59)$$

The q integral is now restricted to the interval $q > 2k$, while $k/q < \cos\theta < 1$. This yields, after performing the ϕ integral as shown in the Appendix,

$$(U, HU) = \frac{1}{4\pi^3\hbar^2 c\rho}\int_0^\infty\frac{d\varepsilon}{v(\varepsilon)^2}\int_{2k}^\infty dq\,(\Xi^2 q^2 + P)$$
$$\times I_{0,0}\left(q, 2\frac{k}{q}\right)\frac{|f^0(\varepsilon_{nk}) - f^0(\varepsilon_{nk} + \sigma\hbar\omega_q)|}{4\sinh^2\left(\hbar\omega_q/2k_BT\right)}, \quad (60)$$

where $I_{0,0}(q, 2k/q)$ is given by Eq. (A5). We may carry out the final integration over energy by expanding the difference of the Fermi functions in powers of ω_q. Since the contribution due to terms involving higher-order derivatives of the Fermi function is seen to vanish by the use of partial integration, we obtain

$$(U, HU) = \frac{1}{2\pi^3\hbar^2 c\rho}\int_0^\infty\frac{d\varepsilon}{v^2(\varepsilon)}\left(-\frac{\partial f^0}{\partial\varepsilon}\right)$$
$$\times\int_{2k}^\infty dq\frac{(\Xi^2 q^2 + P)I_{0,0}(q, 2k/q)\hbar\omega_q}{4\sinh^2\left(\hbar\omega_q/2k_BT\right)}. \quad (61)$$

The remaining steps are standard. We assume that the temperature is much less than the Fermi temperature, so that the integral over ε yields $1/v_F^2$, while k may be replaced by the Fermi momentum k_F. Furthermore, we assume that the temperature is small compared to the characteristic temperature Θ defined by

$$k_B \Theta = \hbar k_F c. \tag{62}$$

Then we obtain

$$(U, HU) = \frac{8}{\pi^2} \frac{m^2 k_F k_B T}{\rho c \hbar^4} \left(\Xi^2 + \frac{P}{4k_F^2} \right)$$
$$\times e^{-2k_F^2 \ell_h^2/(1+\gamma)} e^{-2\Theta/T}. \tag{63}$$

This results in the final conductivity expression

$$\sigma = \frac{2e^2}{h} l_\sigma, \tag{64}$$

where the length l_σ is given by

$$l_\sigma = \frac{\pi c \hbar^3 \rho k_F}{m^2 (4k_F^2 \Xi^2 + P)} e^{2k_F^2 \ell_h^2/(1+\gamma)} e^{2\Theta/T}. \tag{65}$$

At low temperatures the conductivity thus increases exponentially, in agreement with the result of the numerical calculation (see Fig. 3). In the presence of impurities, as we shall see in Sec. V C, the scattering against phonons yields a contribution to the inverse conductivity which is proportional to T^3 rather than $\exp(-2\Theta/T)$, provided the temperature is sufficiently low that the impurities dominate the scattering.

C. Scattering from acoustical phonons and impurities

When the impurity scattering dominates we may use the variational principle with a trial function which is proportional to the solution for impurity scattering alone. We shall consider the case where only the lowest Landau level $n = 0$ is important. The trial function is thus chosen to be proportional to $1/B_{0+}^{0-}$ as given by Eq. (36),

$$U(k) = k^2 \exp \left(2k^2 l_h^2 / [1 + \gamma] \right). \tag{66}$$

Since we have chosen the exact solution to the impurity problem as our trial function, the calculated upper bound on the contribution from electron-phonon scattering $1/\sigma_{ph}$ is exact, to lowest order in the magnitude of the electron-phonon coupling. At low temperatures we may make the approximation

$$[U(k) - U(k')]^2 \simeq \left(\frac{dU(k)}{dk} \right)^2 (k - k')^2, \tag{67}$$

which is justified, since $k - k' = q_x$ and the restriction to low temperatures implies that the phonon momentum is small. Furthermore, we may neglect the deformation-potential coupling since the piezoelectric coupling dominates for small q according to Eq. (53), and also set the

matrix element appearing in Eq. (53) equal to unity. By inserting U in Eq. (26) and carrying out the integrals we obtain

$$\sigma_{ph}^{-1} = \frac{h}{2e^2} l_{ph}^{-1} \frac{3\zeta(3)}{8\pi} \frac{1 + \gamma}{\gamma \tilde{\varepsilon}_F^3} \left(1 + \frac{4\tilde{\varepsilon}_F}{\gamma} \right)^2 \left(\frac{k_B T}{\hbar \omega_h} \right)^3, \tag{68}$$

where $\tilde{\varepsilon}_F = \varepsilon_F / \hbar \omega_h$, and

$$l_{ph}^{-1} = \frac{Pm^*}{\rho c^2 \hbar^2}. \tag{69}$$

This T^3 behavior agrees well with our numerical calculations in the parameter range where it is expected to apply. In Figs. 3 and 4 we show the calculated conductivity, obtained by numerical solution of the integral equation, for samples with different amounts of impurities.
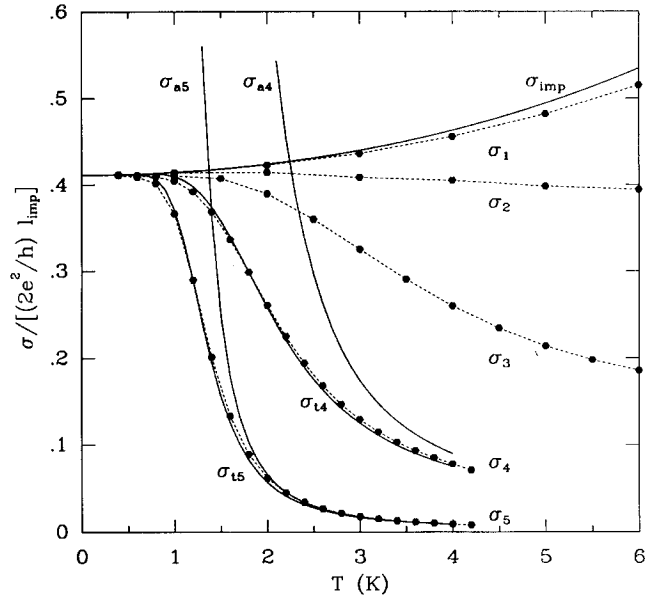

FIG. 3. Plots of the normalized conductivity vs temperature for a GaAs quantum wire at the magnetic field $B = 9$ T, the confinement parameter $\gamma = 0.5$, and the Fermi level $\varepsilon_F = 0.6\hbar\omega_h$. Taking into account both impurity scattering, Eq. (35), and acoustical-phonon scattering, Eqs. (46) and (53), the five dotted curves, $\sigma_1, \ldots, \sigma_5$, are numerical results for the zero-field, zero-temperature mobilities, $\mu_{imp} = 7.5, 75, 300, 3000$, and $30\,000$ m^2/(V s), respectively. The last two rather unrealistic high mobilities are considered to allow a study of the transition from impurity-dominated scattering to phonon-dominated scattering at temperatures low enough [$T < \Theta \simeq 4.0$ K—see Eq. (62)] for the approximative result Eq. (64) to apply. The two full curves σ_{a4} and σ_{a5} are plots of the conductivity (rescaled to match σ_4 and σ_5) calculated from Eq. (64) where only the acoustical-phonon scattering is present. The full curve σ_{imp} is the case where only impurity scattering is present. The two full curves σ_{t4} and σ_{t5} are the results of assuming that the inverse conductivities for each scattering mechanism considered separately may be added, $\sigma_{tj} = \sigma_{aj}\sigma_{imp}/(\sigma_{aj} + \sigma_{imp})$ ($j = 4, 5$), to approximate the exact numerical calculations of the total conductivity.
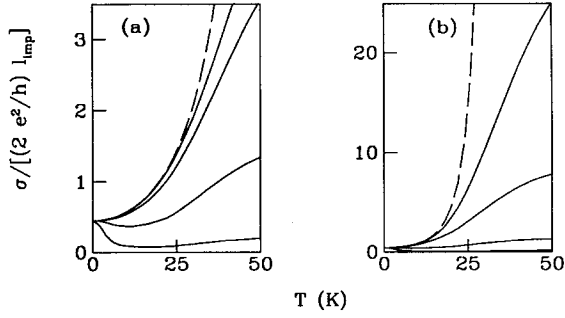
FIG. 4. Plots of the normalized conductivity vs temperature for a GaAs quantum wire at the magnetic field $B = 9$ T and the Fermi level $\varepsilon_F = 0.6\hbar\omega_h$. The confinement parameter in panel (a) is $\gamma = 1.0$ and in (b) it is $\gamma = 0.5$. The dashed curve in each panel is the case where only impurity scattering is taken into account. The four full curves in each panel are the result of combining impurity and acoustical-phonon scattering for each of the following values of the zero-field, zero-temperature mobility $\mu_{imp} = 0.9$, 9, 90, and 900 m^2/(V s).

VI. SCATTERING FROM OPTICAL PHONONS

Next we investigate the combined effects of scattering by longitudinal-optical phonons[19] and impurities. The chief differences from the preceding section involve the q dependence of the electron-phonon matrix element and the absence of dispersion in the phonon frequencies. The conductivity is obtained by solving the Boltzmann equation in the limit where the temperature is much less than $\hbar\omega_0/k_B$.

A. Coupling to optical phonons

We shall use the simple model where the phonon frequency is independent of momentum,

$$\omega_q \simeq \omega_0. \tag{70}$$

The electron-phonon matrix element[19] is given by

$$|g(nn',\mathbf{q})|^2 = \frac{1}{q^2}\frac{M_0^2}{V}M_n^{n'}(u), \tag{71}$$

where V is the normalization volume and where

$$M_0^2 = 2\pi\frac{e^2\hbar\omega_0}{\varepsilon_0}\left(\frac{1}{\kappa_\infty} - \frac{1}{\kappa_0}\right). \tag{72}$$

The function M is given by

$$M_n^{n'}(u) = |\langle nk|e^{i\mathbf{q}\cdot\mathbf{r}}|n'k'\rangle|^2, \tag{73}$$

which is calculated in the Appendix, where also u is defined.

The approximation in Eq. (70) allows us to integrate over the y and z components of the phonon momentum. Using a δ function for the wave function in the z direction, we get

$$\sum_{q_yq_z}|g(nn',\mathbf{q})|^2 = \frac{M_0^2}{(2\pi)^2L}K_n^{n'}(q_x), \tag{74}$$

where

$$K_n^{n'}(q_x) = \int_{-\infty}^{\infty}\frac{dq_y}{\sqrt{q_x^2 + q_y^2}}M_n^{n'}[u(q_x,q_y)]. \tag{75}$$

B. Scattering from optical phonons and impurities

We now consider the case of impurity and optical-phonon scattering. The Boltzmann equation in this case reads

$$\frac{eE_x}{k_BT}v_{nk}f_{nk}^0(1 - f_{nk}^0) = \left(\frac{\partial f_{nk}}{\partial t}\right)_{coll}^{imp} + \left(\frac{\partial f_{nk}}{\partial t}\right)_{coll}^{op}. \tag{76}$$

The collision integral for the phonon scattering given in Eq. (46) simplifies in the case of optical phonons to

$$\left(\frac{\partial f_{nk}}{\partial t}\right)_{coll}^{op} = -\frac{M_0^2}{\hbar 2\pi L}\frac{1}{4\sinh^2(\hbar\omega_0/2k_BT)}\sum_{n'q_x}\sum_\sigma K_n^{n'}(q_x)\left|f^0(\varepsilon_{nk}) - f^0(\varepsilon_{nk} + \sigma\hbar\omega_0)\right|$$
$$\times (\psi_{nk} - \psi_{n'k-q_x})\delta(\varepsilon_{n'k-q_x} - \varepsilon_{nk} - \sigma\hbar\omega_0), \tag{77}$$

with $K_n^{n'}(q_x)$ given in Eq. (75). The argument of the energy-conserving δ function is zero for

$$q_x = k\left(1 - s\sqrt{1 + \frac{\hbar\omega_h(n - n') + \sigma\hbar\omega_0}{\hbar^2k^2/2m}}\right), \tag{78}$$

for each value of nk, provided the square root is real. The branch index s assumes the values $+1$ and -1 corresponding to forward and backward scattering. The Boltzmann equation now simplifies to

$$1 = \sum_{n's'}B_{n+}^{n's'}(\varepsilon)[\phi_n(\varepsilon) - s'\phi_{n'}(\varepsilon)]$$
$$+ \sum_{n's'}C_{n+}^{n's'}(\varepsilon,\sigma)[\phi_n(\varepsilon) - s'\phi_{n'}(\varepsilon + \sigma\hbar\omega_0)], \tag{79}$$

where the matrix B is given by Eq. (36). The optical-phonon scattering gives rise to the matrix C, which is given by

$$C_{ns}^{n's'}(\varepsilon, \sigma) = \frac{1}{f^0(\varepsilon)[1 - f^0(\varepsilon)]} \frac{M_0^2}{\hbar^2 (2\pi)^2} \frac{1}{4 \sinh^2(\hbar\omega_0 / 2k_B T)}$$

$$\times \sum_{\sigma} |f^0(\varepsilon) - f^0(\varepsilon + \sigma\hbar\omega_0)| \frac{K_n^{n'}[sk_n(\varepsilon) - s'k_{n'}(\varepsilon + \sigma\hbar\omega_0)]}{v_n(\varepsilon)v_{n'}(\varepsilon + \sigma\hbar\omega_0)}. \tag{80}$$

In GaAs the typical optical-phonon energies are about 36 meV. Furthermore, since the cyclotron energy $\hbar\omega_c$ in GaAs is 1.5 meV B/T, the typical situation will be that the energy spacing between the Landau levels as modified by the confinement potential $\hbar\omega_h$ is much smaller than the phonon energies $\hbar\omega_0 \gg \hbar\omega_h$. Since we are interested in temperatures that are small or comparable in magnitude to the energy spacing $\hbar\omega_h$, we are therefore always in a situation where $k_B T$ is much less than $\hbar\omega_0$. Under these circumstances it is possible to simplify the Boltzmann equation for electrical transport by considering it to be a coupled system of equations for the functions $\phi(\varepsilon \pm n\hbar\omega_0)$ with n integer. Since the current is mainly determined by the distribution of electrons $\phi(\varepsilon)$ within a thermal layer of thickness comparable to $k_B T$, it is sufficiently accurate to neglect the contribu-

tions from $\phi(\varepsilon \pm n\hbar\omega_0)$, when n is different from zero. The collision integral may therefore be approximated by the "scattering-out" term, corresponding to the neglect of vertex corrections in the Kubo approach.

In calculating the conductivity from Eq. (79) we thus neglect the "scattering-in" terms involving $\phi_{n'}(\varepsilon + \sigma\hbar\omega_0)$, while retaining the full collision matrix for the impurities. We have then evaluated the solution of Eq. (79) numerically and inserted the solution in the conductivity formula (18). Results are shown in Fig. 5. The low-temperature behavior is dominated by the impurities, which give rise to an initial increase of the conductivity, in accordance with Eq. (38). The optical phonons come in at higher temperatures, yielding a maximum of the conductivity as a function of temperature. The position of the maximum is roughly proportional to the logarithm of the strength of the impurity scattering, since the phonon contribution depends exponentially on temperature. Note, however, that the acoustical phonons have reduced the conductivity for the high mobility cases rather strongly at the temperature range shown here; see Fig. 4. The dashed line represents the conductivity without optical phonon scattering.

In comparing the curves in Figs. 3–5 we observe that the optical-phonon scattering in clean systems tends to dominate the total scattering already at fairly low temperatures, around 50 K. This is in contrast to the situation in typical GaAs-based two-dimensional electron gases,[22] where the optical-phonon scattering begins to dominate around 100 K. This effect originates in the increased phase space for scattering in one dimension, caused by the fact that only the x component of the momentum is conserved in the scattering process, while Eq. (75) includes contributions from all perpendicular components q_y.
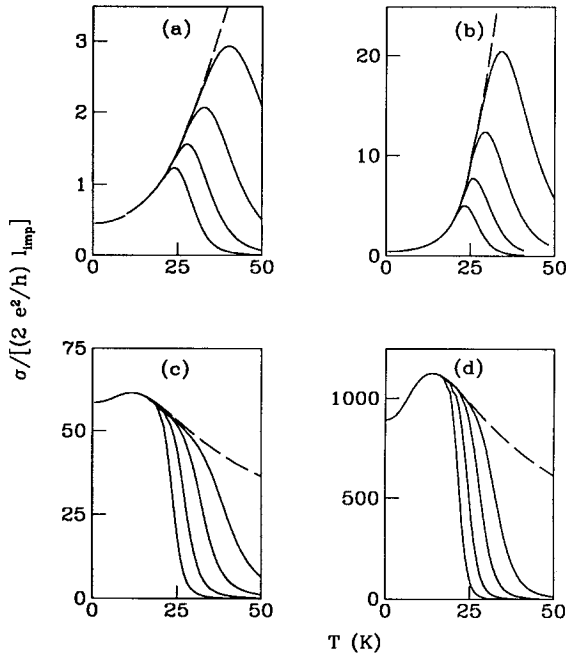

FIG. 5. The conductivity with combined impurity and optical phonon scattering for a GaAs quantum wire. The normalized conductivity is plotted vs temperature for different choices of confinement potential strengths, Fermi energies, and mobilities. The magnetic field is $B = 9$ T. The confinement parameter is $\gamma = 1$ for panels (a) and (c) and $\gamma = 0.5$ for (b) and (d); the Fermi level is $\varepsilon_F = 0.6\hbar\omega_h$, i.e., close to the bottom of the first band, for (a) and (b), and panel (c) and (d) have $\varepsilon_F = 1.3\hbar\omega_h$. The conductivity is shown for each of the following values of the zero-field, zero-temperature mobility, $\mu_{imp} = 0.9, 9, 90$, and 900 m^2/(V s). The dashed curve in each panel is the case where only impurity scattering is taken into account.

VII. CONCLUSION

We have shown that the magnetoconductivity of quantum wires may be discussed in a simple and unified fashion within the framework of a Boltzmann equation, by taking into account the influence of the magnetic field on the electron group velocity and the matrix elements governing the transition probability. By treating in detail the scattering from acoustical as well as optical phonons in the presence of impurity scattering, we have determined the temperature dependence of the magnetoconductivity for realistic choices of parameters in GaAs-based structures. In particular, we have found that the magnetoconductivity exhibits a maximum as a function of temperature, depending on the relative strength of the impurity and electron-phonon scattering. The calculated

magnetoconductivity oscillates when the Fermi energy or the magnetic field is varied. Our detailed calculations show that the scattering against optical phonons in quantum wires is significant at temperatures somewhat smaller than the corresponding temperatures for the two-dimensional case.

We have found that the inverse of the sum of the inverse conductivities (the Matthiessen conductivity) in general is not a good approximation to the total conductivity. If the impurity scattering dominates, the temperature dependence of the electron-phonon contribution is changed from exponential to power-law behavior; cf. Eqs. (65) and (68). If the different scattering contributions are of comparable magnitude the Matthiessen conductivity overestimates the total conductivity with up to a factor of 2 dependent on parameter values. This overestimation is in accordance with the general *resistivity* theorem[18] for the Boltzmann equation: $\rho_{tot} \geq \rho_1 + \rho_2$. Only in the case where the phonon scattering dominates we find a good agreement between the Matthiessen conductivity and the total conductivity; cf. Fig. 3.

In order to address the existing experiments[24–26] more thoroughly a treatment including a calculation of not only the longitudinal conductivity but also the Hall conductivity is in demand.

The effects predicted in this paper should be observable in quantum wires of sufficient purity, since otherwise the electron density may vary considerably due to fluctuations in the electrostatic potential from the donors.

ACKNOWLEDGMENTS

APPENDIX

In this appendix we study the square of the matrix element $\langle nk| \exp(i\mathbf{q}\cdot\mathbf{r})|n'k'\rangle$. Using the single-electron wave functions in Eq. (2) and performing the x and y integrals one obtains

$$|\langle nk| \exp(i\mathbf{q}\cdot\mathbf{r})|n'k'\rangle|^2 = \delta_{k,k'+q_x}\frac{n_{\min}!}{n_{\max}!}u^{|n-n'|}$$
$$\times \left[L_{n_{\min}}^{|n-n'|}(u)\right]^2 e^{-u}, \quad (A1)$$

where $n_{\min} = \min(n,n')$ and $n_{\max} = \max(n,n')$; $L_n^m(u)$ are the Laguerre polynomials while u is given by

$$u = \frac{1}{1+\gamma}\frac{1}{2}(q_x\ell_h)^2 + \frac{1}{2}(q_y\ell_h)^2. \quad (A2)$$

The Kronecker δ function appearing in Eq. (A1), and which is written explicitly in the expression for the integral operator H in Eq. (44), is a consequence of the translational invariance along the x direction.

In calculations involving acoustical phonons it is natural to use the polar coordinates (q,θ,ϕ) with the x axis as the polar axis so that $q_x = q\cos\theta$, $q_y = q\sin\theta\cos\phi$, and $q_z = q\sin\theta\sin\phi$. According to Eqs. (44) and (53) the only ϕ dependence is through u defined above. It is therefore of interest to calculate the integral

$$I_{n,n'}(q,\cos\theta) \equiv \int_0^{2\pi} d\phi\, u^{|n-n'|}\left[L_{n_{\min}}^{|n-n'|}(u)\right]^2 e^{-u}. \quad (A3)$$

From Eq. (A2) it follows that the ϕ dependence of u is of the form $u = \beta + \alpha\cos^2\phi$, so the integrand of $I_{n,n'}$ therefore takes the form of a polynomial in $\cos^2\phi$ times $\exp(-\alpha\cos^2\phi)$. The integral over ϕ may then be carried out explicitly in terms of the beta function and Gauss's hypergeometric function.

In the case where we consider only the lowest Landau level we just need to calculate $I_{0,0}$. Using the results quoted above we find

$$I_{0,0}(q,q_x/q) = 2\pi\exp\left(-\frac{1}{2}(q_x\ell_h)^2\frac{1}{1+\gamma} - \frac{1}{4}\ell_h^2(q^2-q_x^2)\right)$$
$$\times I_0\left(\frac{1}{4}\ell_h^2(q^2-q_x^2)\right) \quad (A4)$$

where $I_0(x)$ is the modified Bessel function of order zero.

[1] For a recent review, see C. W. J. Beenakker and H. van Houten, Solid State Phys. **44**, 1 (1991).
[2] T. Martin and S. Feng, Phys. Rev. Lett. **64**, 1971 (1990); Phys. Rev. B **44**, 9084 (1991).
[3] D. L. Maslov, Y. B. Levinson, and S. M. Badalian, Phys. Rev. B **46**, 7002 (1992).
[4] S. Komiyama, H. Hirai, M. Ohsawa, Y. Matsuda, S. Sasa, and T. Fujii, Phys. Rev. B **45**, 11085 (1992).
[5] H. Akera and T. Ando, Phys. Rev. B **41**, 11967 (1990).
[6] R. Kubo, J. Phys. Soc. Jpn. **12**, 570 (1957).
[7] P. Vasilopoulos, P. Warmenbol, F. M. Peeters, and J. T. Devreese, Phys. Rev. B **40**, 1810 (1989).
[8] N. Mori, H. Momose, and C. Hamaguchi, Phys. Rev. B **45**, 4536 (1992).
[9] H. Bruus and K. Flensberg, J. Phys. Condens. Matter **4**, 9131 (1992).
[10] H. C. Tso and P. Vasilopoulos, Phys. Rev. B **44**, 12952 (1991).
[11] I. I. Boiko, P. Vasilopoulos, and V. I. Sheka, Phys. Rev. B **46**, 7794 (1992).
[12] M. Wagner, Phys. Rev. B **45**, 11606 (1992).
[13] R. Landauer, Philos. Mag. **21**, 768 (1970).
[14] M. Büttiker, Phys. Rev. Lett. **57**, 1761 (1986).
[15] K. Shepard, Phys. Rev. B **44**, 9088 (1991).
[16] M. Suhrke and S. Wilke, Phys. Rev. B **46**, 2400 (1992).
[17] A. A. M. Staring, H. van Houten, C. W. J. Beenakker, and C. T. Foxon, Phys. Rev. B **45**, 9222 (1992).
[18] For a discussion of the Boltzmann equation see, for in-

stance, Henrik Smith and H. Højgaard Jensen, *Transport Phenomena* (Oxford University Press, Oxford, 1989).

[19] G. D. Mahan, in *Polarons in Ionic Crystals and Polar Semiconductors*, edited by J. T. Devreese (North-Holland/American Elsevier, Amsterdam, 1972), p. 553.

[20] P. J. Price, Surf. Sci. **113**, 119 (1982); **143**, 145 (1984).

[21] E. E. Mendez, P. J. Price, and M. Heiblum, Appl. Phys. Lett. **45**, 294 (1984).

[22] W. Walukiewicz, H. E. Ruda, J. Lagowski, and H. C. Gatos, Phys. Rev. B **29**, 4818 (1984).

[23] J. D. Zook, Phys. Rev. **136**, A869 (1964).

[24] A. B. Fowler, A. Hartstein, and R. A. Webb, Physica **117-118B**, 661 (1983).

[25] M. A. Kastner, S. B. Field, J. C. Licini, and S. L. Park, Phys. Rev. Lett. **60**, 2535 (1988).

[26] R. Mottahedeh, M. Pepper, R. Newbury, J. A. A. J. Perenboom, and K.-F. Berggren, Solid State Commun. **72**, 1065 (1989).

[27] J. S. Blakemore, J. Appl. Phys. **53**, R123 (1982)